Acta Crystallographica Section D
Biological Crystallography
ISSN 0907-4449

pH-dependent structural changes in haemoglobin component V from the midge larva *Propsilocerus akamusi* (Orthocladiinae, Diptera)

Takao Kuwada,[a]* Tomokazu Hasegawa,[b] Takashi Takagi,[c]‡ Isamu Sato[a,d] and Fumio Shishikura[a,e]

[a]Laboratory for Electron Beam Research and Application (LEBRA), Institute of Quantum Science, Nihon University, Funabashi, Chiba 274-8501, Japan, [b]Rigaku Co., Akishima, Tokyo 196-8666, Japan, [c]Graduate School of Life Sciences, Tohoku University, Sendai, Miyagi 980-8578, Japan, [d]Advanced Research Institute for the Science and Humanities, Nihon University, Chiyoda-ku, Tokyo 102-8251, Japan, and [e]Department of Chemistry, Nihon University School of Medicine, Itabashi-ku, Tokyo 173-8610, Japan

‡ Present address: Peptide Door Co. Ltd, Takasaki, Gunma 370-0854, Japan.

Correspondence e-mail: kuwadat@lebra.nihon-u.ac.jp

Received 6 November 2009
Accepted 30 December 2009

PDB References: haemoglobin component V, pH 4.6, 2zwj; pH 5.6, 3a5a; pH 6.5, 3a5b; pH 7.0, 3a5g; pH 9.0, 3a9m.

Haemoglobin component V (Hb V) from the midge larva *Propsilocerus akamusi* exhibits oxygen affinity despite the replacement of HisE7 and a pH-dependence of its functional properties. In order to understand the contribution of the distal residue to the ligand-binding properties and the pH-dependent structural changes in this insect Hb, the crystal structure of Hb V was determined under five different pH conditions. Structural comparisons of these Hb structures indicated that at neutral pH ArgE10 contributes to the stabilization of the haem-bound ligand molecule as a functional substitute for the nonpolar E7 residue. However, ArgE10 does not contribute to stabilization at acidic and alkaline pH because of the swinging movement of the Arg side chain under these conditions. This pH-dependent behaviour of Arg results in significant differences in the hydrogen-bond network on the distal side of the haem in the Hb V structures at different pH values. Furthermore, the change in pH results in a partial movement of the F helix, considering that coupled movements of ArgE10 and the F helix determine the haem location at each pH. These results suggested that Hb V retains its functional properties by adapting to the structural changes caused by amino-acid replacements.

1. Introduction

The His residue at the E7 helical position is highly conserved in many haemoglobin (Hb) and myoglobin (Mb) components and plays an important role in the functional properties of these components (Ikeda-Saito *et al.*, 1978; Phillips, 1980; Phillips & Schoenborn, 1981; Shaanan, 1983; Fann *et al.*, 1995). The HisE7 residue on the distal side of haem acts as a proton donor to stabilize the ligand bound to a haem iron; therefore, genetic substitution of the His by nonpolar residues leads to a significant decrease in ligand affinity (Olson *et al.*, 1988; Rohlfs *et al.*, 1990; Springer *et al.*, 1994). However, some members of the haemoglobin superfamily exhibit relatively high oxygen affinity despite the natural substitution of HisE7 by polar (Yang *et al.*, 1995; Mito *et al.*, 2002) as well as nonpolar residues (Bolognesi *et al.*, 1990, 1997; Mattevi *et al.*, 1991; Conti *et al.*, 1993; Milani *et al.*, 2001; Ouellet *et al.*, 2006). In the case of Nematoda Hb, in which the HisE7 residue is replaced by a polar Gln, GlnE7 and Tyr at the B10 helical position form hydrogen bonds to the ligand and together grip the ligand in the haem-binding pocket (Yang *et al.*, 1995). In cases in which the HisE7 residue in globin proteins is replaced by a nonpolar residue, the functional properties are controlled by one or more distal residues other than the E7 residue, for example, ArgE10 in mollusc Mb (Bolognesi *et al.*, 1990; Mattevi *et al.*, 1991; Conti *et al.*, 1993) and TyrB10 and/or GlnE11 in bacterial

truncated Hb (trHb; Milani *et al.*, 2001; Ouellet *et al.*, 2006). These results suggest that the ligand-binding properties are controlled by various stereochemical mechanisms in the haemoglobin superfamily and different structural changes have been developed as oxygen-transport mechanisms during the evolution of these globins (Bolognesi *et al.*, 1990, 1997; Mattevi *et al.*, 1991).

Propsilocerus akamusi (old species name *Tokunagayusurika akamusi*) is a common species of midge found in eutrophic lakes in Japan. Hb from the fourth-instar midge larva of this species is composed of at least 11 different components (Fukuda *et al.*, 1993). These Hb components have been classified into two distinct types on the basis of their spectroscopic properties, low absorbance (L-type) and normal absorbance (N-type), which were found to exist in monomeric and dimeric forms, respectively. Components V (Hb V) and VII (Hb VII) are representatives of the L-type and the N-type, respectively. The structural and functional features of these components have been examined in previous studies (Fukuda *et al.*, 1993; Akiyama *et al.*, 1994; Koshikawa *et al.*, 1998; Kamimura *et al.*, 2003; Yamamoto *et al.*, 2003; Kuwada *et al.*, 2007). One of the most remarkable differences between the two components is the replacement of HisE7 by a nonpolar Ile in Hb V. Kamimura *et al.* (2003) demonstrated that despite this replacement Hb V exhibits oxygen affinity and a Bohr effect similar to those observed in mammalian Mbs. They further predicted that PheB10 stabilizes the bound O_2 in Hb V. However, paramagnetic proton nuclear magnetic resonance (H-NMR) studies on methaemoglobin (met-Hb) V indicated the characteristic OH^- and Cl^- affinities to be pH-dependent and suggested that the side chain of ArgE10 acts as a proton donor for these ligands in the protein (Koshikawa *et al.*, 1998; Yamamoto *et al.*, 2003). In order to understand the structural features of the Hb components in insects, we have previously determined the crystal structures of Hb V and Hb VII from *P. akamusi* (Kuwada *et al.*, 2007). Structural comparison of these Hb components indicated that Hb V has an additional helix at the C-terminal region, although Hb VII has a normal globin fold composed of eight helices, and the haem geometry in ligated Hb V differs from that in typical globin proteins. However, because the apparent interactions between the ligand and the distal residues could not be observed in Hb V, the contribution of the distal residues to ligand binding remains unknown.

Changes in the pH have a significant effect on the functional properties of Hb V, such as the Bohr effect and the anionic ligand affinity (Koshikawa *et al.*, 1998; Kamimura *et al.*, 2003; Yamamoto *et al.*, 2003). The pH-dependence of its functional properties indicates that Hb V exhibits pH-dependent structural changes; therefore, crystallographic analysis of the protein at a given pH alone would not provide sufficient structural information (Kuwada *et al.*, 2007). In fact, vertebrate Hbs have been reported to show significant structural changes with varying pH, with a consequent contribution to ligand affinity (Robinson *et al.*, 2003; Yokoyama *et al.*, 2004). Therefore, comparing the Hb V structures under various pH conditions might provide useful clues for understanding its structure–function properties (Koshikawa *et al.*, 1998). In this study, we determined the crystallographic structures of Hb V under two acidic conditions (pH 4.6 and 5.6), two neutral conditions (pH 6.5 and 7.0) and one alkaline condition (pH 9.0). On the basis of these Hb V structures, we describe the contribution of the distal residue to the ligand-binding properties and the pH-dependent structural changes in the haem region, which can affect the functional properties of the Hb component.

2. Materials and methods

2.1. Crystallization

We purified Hb V from fourth-instar midge larvae of *P. akamusi*, as described by Fukuda *et al.* (1993). The Hb solution was reduced using 10 m*M* sodium dithionite in 0.1 *M* Tris–HCl pH 7.5 and was converted to the carbonmonoxy form by gently bubbling CO gas. Crystallization was carried out by the hanging-drop vapour-diffusion technique at 293 K. We prepared the following crystallization solutions with different pH values to investigate the pH-dependent structural changes in Hb V: 22.5–25% PEG 3350 in 0.1 *M* sodium acetate buffer pH 4.6 and pH 5.6, 22.5–25% PEG 3350 in 0.1 *M* bis-tris buffer pH 6.5 and 22.5–25% PEG 3350 in 0.1 *M* Tris–HCl buffer pH 7.0 and pH 9.0. The crystallization solutions did not contain salts because it is possible that salts may affect the structure of Hb V. The crystals were grown in a drop containing protein solution (approximately 10 mg ml^{-1}) mixed with an equal amount of each of the crystallization solutions. The crystallization solutions were degassed and purged with CO gas before use and all crystallizations were set up under an atmosphere of nitrogen in a glove bag. The wells of the crystallization plates were filled with CO and the plates were sealed in bags and placed in the dark. The crystals grown in solutions at acidic and neutral pH values appeared after 3–5 d. In contrast, the crystals from the solution at pH 9.0 formed over a period of roughly six months.

Surplus Hb V crystals that were not suitable for use in the X-ray diffraction analyses were spectroscopically analyzed to check the ligand states of the crystal under each pH condition. Hb V crystals grown under each pH condition were picked up from the crystallization drop and dissolved in 5 µl 0.1 *M* buffer solutions adjusted to each crystallization pH. Solutions containing dissolved crystals were purged using nitrogen gas and kept at 253 K until the spectroscopic measurements were performed. The absorption spectra were measured in the UV–Vis region using a NanoDrop ND-1000 spectrophotometer.

2.2. X-ray diffraction analyses

X-ray diffraction data for each crystal were collected at 100 K using Cu $K\alpha$ wavelength X-rays from a rotating-anode X-ray generator (Rigaku UltraX 18) and an imaging-plate detector (Rigaku R-AXIS IV^{++}). For X-ray data collection, the crystals were soaked in a cryoprotectant solution containing 30% PEG 3350 or 10% glycerol before flash-freezing them in a nitrogen stream. Diffraction data for Hb V crystals

Table 1
Data-collection and refinement statistics.

Values in parentheses are for the highest resolution shell.

	pH 4.6	pH 5.6	pH 6.5	pH 7.0	pH 9.0
Diffraction data					
Space group	$P2_12_12$	$P2_12_12$	$P2_12_12_1$	$P2_12_12_1$	$P2_12_12_1$
Unit-cell parameters					
a (Å)	65.54	65.49	33.34	33.51	33.58
b (Å)	75.26	75.17	63.61	64.14	64.51
c (Å)	33.68	33.61	72.04	72.66	72.82
Resolution (Å)	49.43–1.81 (1.87–1.81)	49.38–1.83 (1.90–1.83)	47.69–1.81 (1.87–1.81)	48.08–1.81 (1.87–1.81)	24.68–1.80 (1.86–1.80)
No. of recorded reflections	214626	205024	197937	99783	209284
No. of unique reflections	15772	15190	14451	14864	15253
Completeness (%)	99.7 (99.9)	99.5 (100.0)	99.2 (98.0)	99.8 (99.9)	100.0 (100.0)
$R_{\rm merge}$† (%)	5.3 (14.7)	4.7 (15.0)	6.2 (19.8)	5.4 (22.9)	4.5 (13.3)
$\langle I/\sigma(I)\rangle$	26.1 (12.1)	31.4 (12.5)	21.3 (9.7)	18.9 (6.1)	34.1 (15.4)
Multiplicity	13.61 (13.19)	13.50 (13.48)	13.70 (13.38)	6.71 (6.62)	13.72 (13.51)
Model statistics					
R factor (%)	0.187	0.189	0.186	0.190	0.204
$R_{\rm free}$ (%)	0.203	0.205	0.197	0.208	0.232
No. of atoms					
Protein	1213	1213	1213	1213	1213
Haem + ligand	43 + 1	43 + 1	43 + 1	43 + 2	43 + 2
Solvent	264	257	188	219	316
R.m.s. deviations					
Bond lengths (Å)	0.011	0.011	0.011	0.019	0.023
Bond angles (°)	1.2	1.3	1.1	1.7	1.7
Mean B factors (Å^2)					
Main-chain atoms	12.9	12.3	17.4	19.7	18.2
Side-chain atoms	15.2	15.7	20.6	22.8	21.5
Haem atoms	16.7	18.2	18.9	21.8	23.4
Ligand atoms	17.2	25.9	12.0	14.4	16.3
Solvent atoms	26.2	26.7	33.5	33.8	36.1
Ramachandran plot‡ (%)					
Most favoured	97.0	97.0	96.2	94.7	95.5
Additional allowed	3.0	3.0	3.8	5.3	4.5

† $R_{\rm merge} = \sum_{hkl}\sum_i |I_i(hkl) - \langle I(hkl)\rangle| / \sum_{hkl}\sum_i I_i(hkl)$. ‡ Stereochemistry was assessed by *PROCHECK* (Laskowski *et al.*, 1993).

grown at pH 4.6, 5.6, 6.5, 7.0 and 9.0 were collected to 1.81, 1.83, 1.81, 1.81 and 1.80 Å resolution, respectively. The diffraction data sets were processed using *CrystalClear* (v.1.3.6; Rigaku Co., Tokyo, Japan). The data-collection and processing parameters of the crystals are summarized in Table 1.

2.3. Refinement and structural analysis

The crystal structure of *P. akamusi* Hb V at each pH was solved at 3.5 Å resolution by the molecular-replacement (MR) method with *CNX* (MSI Inc., California, USA). The search model used was the previously determined structure of Hb V (PDB entry 1x3k; Kuwada *et al.*, 2007). To generate the search model, the residues of the haem pocket (18 amino-acid residues) were replaced with Ala and the haem group and all solvent atoms were removed. The MR models were refined using *CNX* functions while increasing the resolution stepwise to the highest resolution. The missing portions of each Hb V model were manually built using *X-BUILD* (*QUANTA*; MSI Inc.) guided by a composite annealed OMIT map. The models were fitted to the electron-density map and refined using *CNX* and *REFMAC* (Winn *et al.*, 2001). Haem and solvent molecules were added after all the amino-acid residues had been modelled. Water molecules were added using *X-SOLVATE* (*QUANTA*; MSI Inc.) guided by $F_o - F_c$ electron-density maps countered at 3σ and manually verified in *X-BUILD*. The quality of the final models was assessed using *PROCHECK* (Laskowski *et al.*, 1993). The refined statistics for all crystal structures are shown in Table 1.

For comparison of the Hb V structures, the Hb V coordinates were superimposed using 92 C^{α} atoms of the B, G and H helices according to the BGH frame (Baldwin & Chothia, 1979). By convention, individual residues were designated by the homologous helical position in sperm whale Mb (Knapp *et al.*, 2005). Thus, we designated Ile66 as the E7 residue, which corresponds to HisE7 in Mb, and His98 as the F8 residue, although Ile66 and His98 are the sixth residue and the 15th residue in the E and F helices of Hb V, respectively (Kuwada *et al.*, 2007). The bond angles and distances between the atoms were measured using *Swiss-PdbViewer* (Guex & Peitsch, 1997) and *CONTACT* (Collaborative Computational Project, Number 4, 1994). The hydrogen bonds were defined by hydrogen-donor and hydrogen-acceptor distances of below 3.6 Å and donor–hydrogen–acceptor angles of above 90° (Krell *et al.*, 1998). Structural figures were drawn using *PyMOL* (DeLano, 2002).

3. Results and discussions

3.1. Refined models

In this study, we determined the crystal structure of *P. akamusi* Hb V at five different pH values (Table 1). Hb V crystals grown under acidic conditions at pH 4.6 and 5.6 belonged to space group $P2_12_12$ with one monomer per asymmetric unit. These crystals were identical to the Hb V crystal grown at pH 4.6 in a previous study (Kuwada *et al.*, 2007). The Hb V models at pH 4.6 and 5.6 were refined at 1.81 Å to an R factor of 0.187 ($R_{\rm free}$ = 0.203) and at 1.83 Å to an R factor of 0.189 ($R_{\rm free}$ = 0.205), respectively. Moreover, Hb V crystals grown in pH 6.5, 7.0 and 9.0 solutions belonged to space group $P2_12_12_1$ with one monomer per asymmetric unit. The unit-cell volume of the $P2_12_12_1$ crystals is 5.6–8.0% smaller than that of the $P2_12_12$ crystals at acidic pH. The Hb V models at pH 6.5, 7.0 and 9.0 were refined at 1.81 Å to an R factor of 0.186 ($R_{\rm free}$ = 0.197), at 1.81 Å to an R factor of 0.190 ($R_{\rm free}$ = 0.208) and at 1.80 Å to an R factor of 0.204

(R_{free} = 0.232), respectively. All five refined Hb V models consisted of a complete polypeptide chain (152 amino-acid residues), one haem group and 188–316 solvent molecules each.

Fig. 1 shows the electron-density maps around the haem group of each refined Hb V model. The electron density at the sixth ligand position of the haem iron was evident in all five structures and enabled identification of the exogenous ligand molecule bound to the haem. Electron density for a diatomic ligand molecule was observed in Hb V at pH 7.0 and 9.0; however, the corresponding electron densities at pH values lower than 7.0 revealed a monatomic ligand despite all the crystallization trials being carried out in the presence of CO. The visible absorption spectra of Hb V at pH 4.6 displayed increased absorption intensities at approximately 510 and 630 nm (Fig. 2); these findings are characteristic of met-Hb (Fukuda *et al.*, 1993), suggesting that the ligand position at pH 4.6 is occupied by a water molecule as in the typical acid met forms of Hb. Although the absorption spectra of Hb V at pH 5.6 and 6.5 were similar to those of the CO form of Hb V at pH 7.0 and 9.0, a water molecule was refined as a ligand molecule in the crystal structures at pH 5.6 and 6.5 because of the size of the electron density.

The overall folds of these Hb V structures are almost identical to one another, with root-mean-square deviations (r.m.s.d.s) of less than 0.60 Å for each pair. A remarkable difference among these structures, particularly between the Hb V structures at neutral pH and at other pH conditions, exists in the haem region as described below. In this study, we succeeded in growing Hb V crystals at five different pH values without adding salts that may affect their structure and without substantially changing the concentration of PEG. The crystallization trials were performed under CO conditions because of concerns regarding ligand-dependent structural changes of Hb V. However, structural analyses indicated the existence of a water molecule at the sixth ligand position at pH values lower than 7.0. Because the difference in the ligand molecule, either CO or water, might complicate the detection of pH-dependent structural changes in the Hb V structures, we performed an additional analysis of an apparent aquomet-Hb V crystal that was grown at pH 6.5 and auto-oxidized in air (unpublished data). The results indicated that the structural characteristics of the aquomet-Hb V crystal (grown at pH 6.5) were similar to those of the other Hb V crystals grown under neutral conditions. Therefore, from the results of this study it can be concluded that the structural differences in the haem region in the Hb structures at neutral and other pH conditions are mainly pH-dependent and are not dependent upon the exogenous ligand molecule and other external factors.

The Hb V structures at different pH conditions also exhibited differences with respect to the backbone in the C-terminal regions. The Hb V structures in acidic and alkaline conditions contained nine helices, eight of which (A–H) were typical of globin proteins and the ninth of which was a short additional helix at the C-terminus that is characteristic of Hb V (Kuwada *et al.*, 2007). At neutral pH, the C-terminal

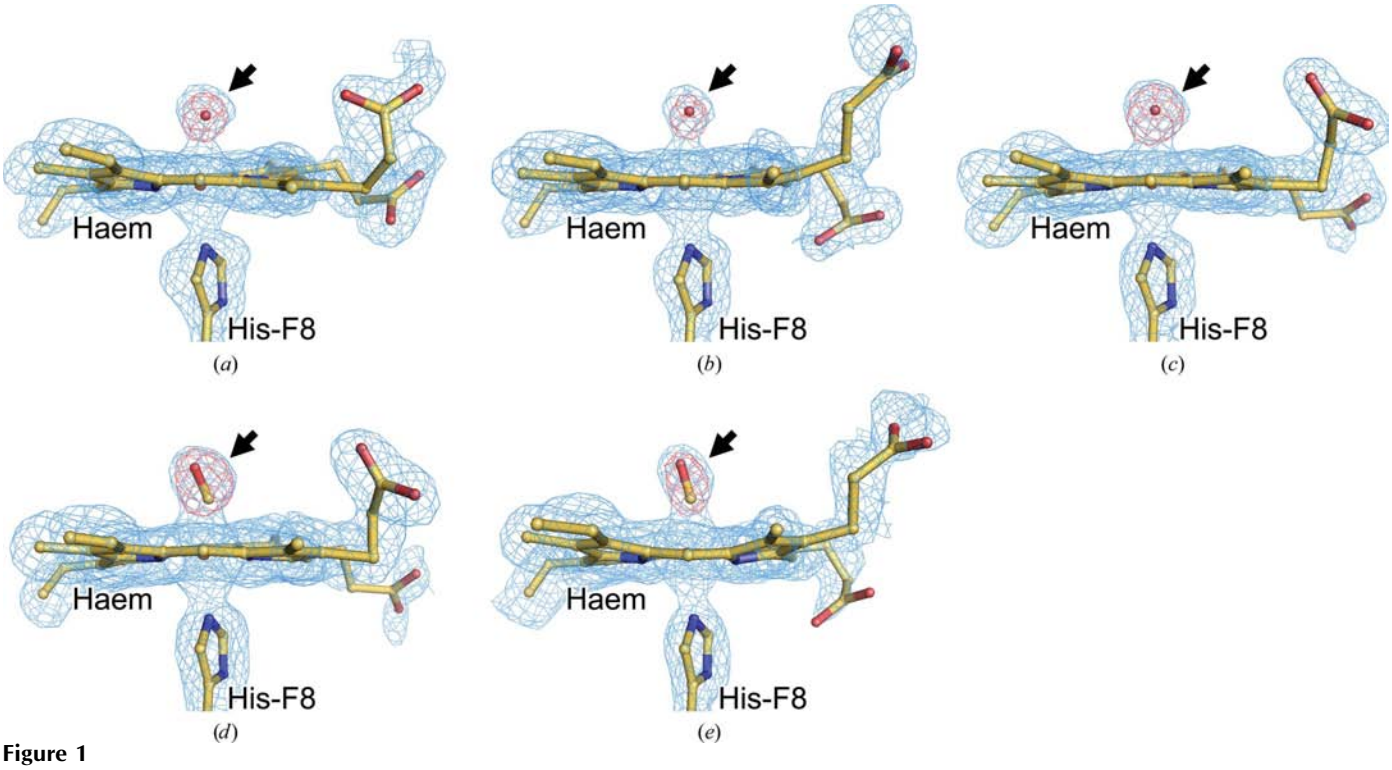

Figure 1
Electron-density maps surrounding the haem region of Hb V at (*a*) pH 4.6, (*b*) pH 5.6, (*c*) pH 6.5, (*d*) pH 7.0 and (*e*) pH 9.0. Arrows indicate the electron densities for the exogenous ligand molecule. The $2F_o - F_c$ composite annealed OMIT maps (sky blue) and $F_o - F_c$ maps (red) are contoured at 1σ and 5σ, respectively. Each map was calculated without ligand molecules. For the ligand molecule, a water molecule was fitted at pH 4.6, 5.6 and 6.5 and a CO molecule at pH 7.0 and 9.0.

region of Hb V contains a hydrogen-bonded turn but not a helix. However, it was uncertain whether the structural change in the C-terminal region is pH-dependent because the aquomet-Hb V at pH 6.5 contained a short C-terminal helix identical to that observed in Hb V under acidic and alkaline conditions. Other differences between the Hb V structures were observed in the N-terminal region and corner regions connecting the helices; however, there are no remarkable associations between these structural differences and the crystallization conditions.

3.2. Swinging movement of ArgE10

Fig. 3 shows the overlapping of all five Hb V structures around the haem region. The orientation of the side chain of ArgE10 on the distal side of the haem differs significantly at different pH values. At both pH 6.5 and 7.0 the Arg side chain lies above the haem plane within a distance of 4 Å and its N^{ε} atom forms a hydrogen bond to the ligand molecule (Fig. 4*b*). In the CO form at pH 7.0, although only a weak hydrogen bond (3.56 Å) was observed between the O atom of the haem-bound CO and the N^{ε} atom of the Arg side chain, the N^{ε} atom simultaneously contacts the C atom of the haem-bound CO at a distance of 3.34 Å. Moreover, the NH of the Arg side chain also appears to grip the ligand molecule with noncovalent bonds. The Arg residue is suggested to form stronger hydrogen bonds to the haem-bound oxygen molecule in oxy Hb V. Incidentally, at pH 6.5 the N^{ε} atom and NH of ArgE10 form hydrogen bonds to the haem-bound water molecule at distances of 3.19 and 3.43 Å, respectively. At acidic and alkaline pH the ArgE10 side chain swings outward from the haem pocket and is exposed to the solvent. Compared with the orientation of the Arg side chain under neutral conditions, the Arg side chain rotates by almost 180° around the $C^{\alpha}-C^{\beta}$ bond at acidic and alkaline pH. Moreover, at acidic pH the Arg side chain rotates by approximately 90° around the $C^{\gamma}-C^{\delta}$ bond compared with that at alkaline pH. Under acidic and alkaline conditions no direct hydrogen bond can be observed between ArgE10 and the haem ligand (Figs. 4*a* and 4*c*).

To understand the functional properties of *P. akamusi* Hb V, it is important to identify the distal residue that functionally compensates for the absence of a polar E7 residue. Structural analyses of Hb V at neutral pH revealed that the Arg residue stabilizes the exogenous ligand molecule through a hydrogen bond. Further, none of the other distal residues made direct contact with the ligand molecule or showed any remarkable conformational differences among the Hb V structures. Previous H-NMR studies have discussed the contribution of ArgE10 to the functional properties of Hb V (Koshikawa *et al.*, 1998; Yamamoto *et al.*, 2003). Our study supported the findings of the above-mentioned studies and is the first study to demonstrate that Arg contributes to ligand binding in Hb V. Furthermore, it was revealed that a change to acidic or alkaline pH causes the swinging movement of the Arg, as a consequence of which its direct hydrogen bond to the ligand molecule is lost.

The role of ArgE10 in ligand binding has previously been examined in the Mb of a mollusc, *Aplysia limacina*, in which the E7 helical position contains a nonpolar Val residue (Bolognesi *et al.*, 1990; Mattevi *et al.*, 1991; Conti *et al.*, 1993). Fig. 5(*a*) illustrates that the location of the ArgE10 side chain of Hb V in the neutral condition is identical to that of the side chain in anionic ligand-binding forms of the mollusc Mb. It should be noted that the hydrogen-bond network between

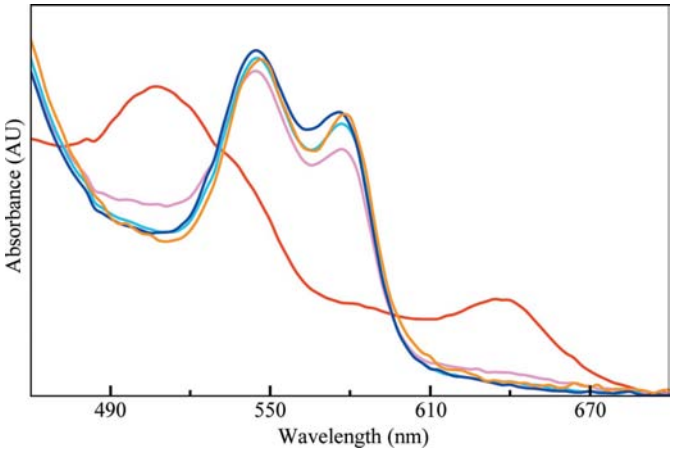

Figure 2
The visible absorption spectra of Hb V at all five pH values. Spectra at pH 4.6, 5.6, 6.5, 7.0 and 9.0 are indicated in red, pink, cyan, blue and orange, respectively. For spectroscopic analysis, surplus crystals were dissolved in 5 µl 0.1 *M* buffer solutions adjusted to each of the five pH values.

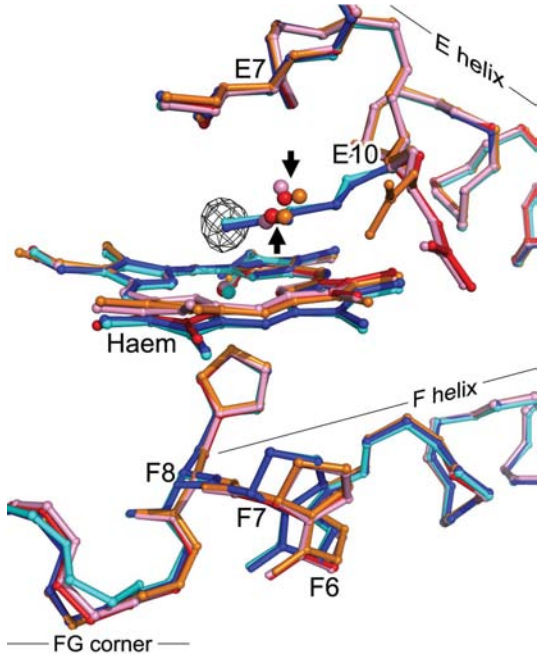

Figure 3
Overlapping of the haem region of the five Hb V structures based on the BGH frame. The pH 4.6, 5.6, 6.5, 7.0 and 9.0 coordinates are indicated in red, pink, cyan, blue, and orange, respectively. Arrows indicate the distal side water molecules in the acidic and alkaline conditions. The positions of the Fe-bound ligand are indicated as a black net to represent the electron density. Except for the numbered residues IleE7, ArgE10, GlyF6, ProF7 and HisF8, the haem regions are displayed as backbone atoms; the propionate groups of the haem have been deleted for easy viewing.

Arg and the haem group in Hb V is almost identical to that in the anionic ligand-bound mollusc Mb. Furthermore, the location of ArgE10 in Hb V under acidic and alkaline conditions is similar to that in the unligand form of mollusc Mb (Fig. 5*b*). In mollusc Mb the Arg side chain points towards the solvent in the deoxy and imidazole-binding forms and folds back towards the distal side of the haem in the presence of the anionic haem-bound ligand (Bolognesi *et al.*, 1990; Mattevi *et al.*, 1991; Conti *et al.*, 1993). Although the unliganded form of Hb V remains unclear, it is possible that the movement of ArgE10 also plays an important role in regulation of ligand dissociation in Hb V.

It is interesting to note that the swinging movement of ArgE10 in Hb V is similar to that in *A. limacina* Mb. Mattevi *et al.* (1991) suggested that ArgE10 has been selected by molecular evolution to grant ligand stabilization in mollusc Mb, which lacks a hydrogen-bond donor residue at the E7 position. Because there are no notable evolutionary relationships between *P. akamusi* Hb V and mollusc Mb, it is inferred that Arg was independently selected in this insect Hb lineage and acquired a function identical to the Arg in the mollusc Mb. In mammalian Mb mutants with replacements of His to Val at the E7 position and Thr to Arg at the E10 position, the Arg residue also directly interacts with the haem-bound ligand (Smerdon *et al.*, 1995). Conformational flexibility of the ArgE10 side chain has also been observed in cytoglobin, a member of the hexacoordinate globin superfamily, implying the participation of the Arg in the ligand binding in this globin (Sugimoto *et al.*, 2004). Moreover, in neuroglobin, a hexacoordinate globin expressed in the nervous system, LysE10 is believed to contribute not only to stabilization of the ligand molecule but also to modulation of the Bohr effect (Couture *et al.*, 2001; Fago *et al.*, 2004). These data suggest that the polar E10 residue observed in various globins plays an important role in maintaining their functional properties according to the physiological conditions.

3.3. Changes in the hydrogen-bond networks on the distal side

Under acidic and alkaline conditions, the space above the haem plane is occupied by two water molecules instead of the long side chain of ArgE10. The swinging movement of ArgE10 and the presence of water molecules above the haem plane induce significant differences in the hydrogen-bond network between the different Hb V structures. As shown in Fig. 4, two hydrogen-bond networks can be observed on the distal side of the haem in each Hb V structure. One of the networks connects the residues at the CD corner to the haem through a water molecule (W1) and another connects the residue at the E helix to the haem group. Although the network between the CD corner and the haem of different Hb V structures does not differ significantly, the differences in the hydrogen-bond network between the E helix and the haem in different Hb structures are noteworthy. In Hb V at neutral pH the ArgE10 side chain directly connects to the haem and the ligand molecule. However, in the cases of Hb V under acidic and alkaline conditions the two water molecules (W2 and W3) above the haem plane contribute to the formation of the hydrogen-bond network between the haem group and the distal side residue in place of the ArgE10 side chain. One of them (W2) bonds with the propionic acid side chain of the haem and/or the ArgE10 side chain, while the other (W3) forms a hydrogen network with the main-chain O atom of IleE7 and the haem-bound ligand molecule.

The presence of the distal side water molecules and their contribution to forming hydrogen-bond networks have been investigated in bacterial Hbs (Tarricone *et al.*, 1997; Milani *et al.*, 2003; Bonamore *et al.*, 2005; Ouellet *et al.*, 2007, 2008). Interestingly, the water molecules on the distal side

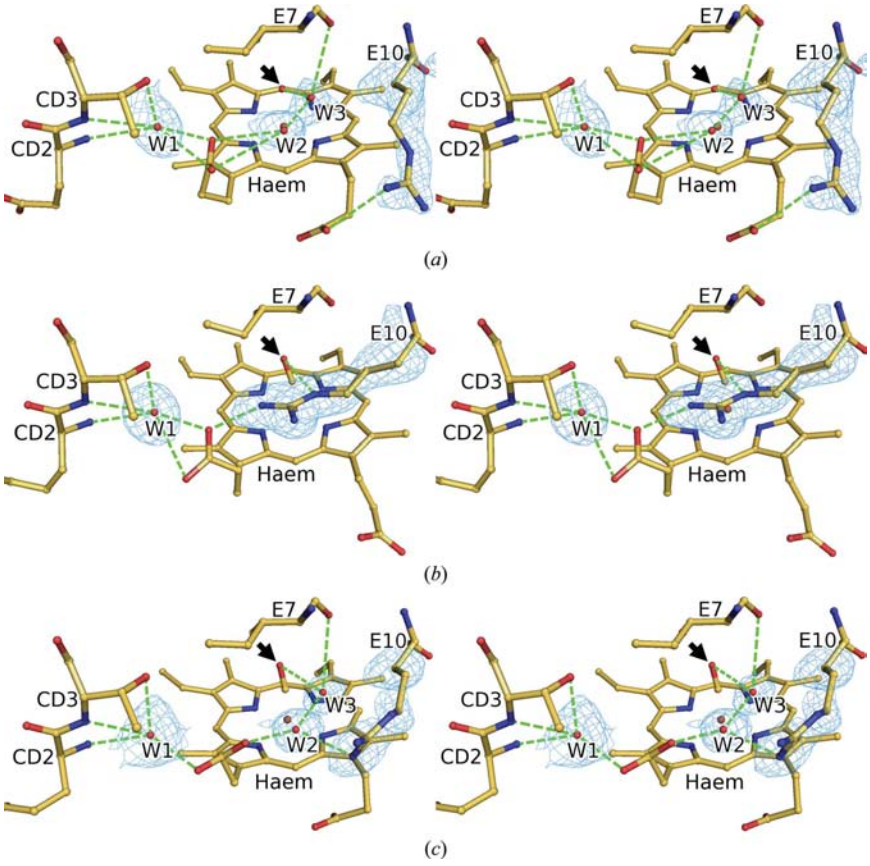

Figure 4
Stereogram of the hydrogen-bond network on the distal side of the haem of the Hb V at pH 4.6 (*a*), pH 7.0 (*b*) and pH 9.0 (*c*). Light-green broken lines represent the hydrogen bonds between the haem groups, the distal side water molecules (W1–W3) and distal residues including Glu (CD2) and Thr (CD3) at the CD corner region. Sky-blue nets are the $F_o - F_c$ maps contoured at 2σ calculated without the ArgE10 side chain and the distal side water molecules. Arrows indicate the exogenous ligand molecule.

of Hb V at acidic and alkaline pH are found in essentially the same positions as those in *Mycobacterium* trHb (Milani *et al.*, 2003; Ouellet *et al.*, 2007, 2008). Ouellet *et al.* (2007) suggested that water molecules at the entrance of the distal side, such as W1 and W2, contribute to further blocking access of gaseous ligands to deoxygenated and oxygenated trHb and a water molecule above the haem plane, such as W3, forms a strong barrier to ligand binding in the absence of the haem-bound diatomic ligand. In a similar study, Olson & Phillips (1996) indicated that stabilization of the noncoordinated water molecule (W3) causes a marked decrease in the association-rate constants for all ligands in deoxy Mb. These data imply that the distal water molecules in Hb V also prevent the undesirable access of ligand molecules to the haem pocket. In particular, W2 and W3 are important constituents of a kinetic barrier for ligand binding under acidic and alkaline conditions because no other residues contribute to the formation of such a barrier under these pH conditions. Further, Hb V displays a unique property: the pH-dependent swinging movement of ArgE10 allows the distal water molecules to exit.

Table 2
Haem geometry of Hb V at varying pH.

	pH 4.6	pH 5.6	pH 6.5	pH 7.0	pH 9.0
Distance (Å)					
Fe—ligand†	2.32	2.45	2.45	1.87 (2.39)	1.88 (2.45)
Fe—Pn‡	0.06	0.06	0.04	0.06	0.14
Fe—F8 $N^{\varepsilon 2}$§	2.17	2.19	2.17	2.20	2.20
F8(C^{δ}—N3) − (C^{e}—N1)¶	0.45	0.42	0.33	0.37	0.40

† The distance between the haem iron and the ligand molecule (water molecule at pH 4.6, 5.6 and 6.5 and the C atom of CO at pH 7.0 and 9.0). The values in parentheses at pH 7.0 and 9.0 indicate the distance between the haem iron and the geometric centre of the CO molecule. ‡ The distance between the haem iron and the centre of the four porphyrin N atoms. § The distance between the haem iron and the N^{e} atom of HisF8. ¶ The difference between the two distances representing a tilting of the imidazole of HisF8. One is between the C^{δ} atom of HisF8 and the N3 atom of porphyrin and the other is between the C^{e} atom of HisF8 and the N1 atom of porphyrin. This tilting links the shift of the F helix towards the FG corner upon ligand binding (Mito *et al.*, 2002). These values are almost identical to those in the known Hb V structure at pH 4.6 (Kuwada *et al.*, 2007).

Yamamoto *et al.* (2003) performed an H-NMR study of the Cl^{-} affinities in Hb V and reported that the propionate group of haem forms a kinetic barrier for Cl^{-} entry into the haem pocket. Our results indicated that the water molecules on the distal side of haem are included in the kinetic barrier. It has been suggested that ArgE10 in met-Hb V contributes to Cl^{-} binding under high salt concentrations at acidic pH (Yamamoto *et al.*, 2003) and OH^{-} binding in alkaline pH (Koshikawa *et al.*, 1998). However, the Arg contribution for the ligand binding is not observed in Hb V structures under acidic and alkaline pH conditions. Under these pH conditions, the distal side water molecules may simultaneously play a role in blocking the access of ligand molecules and temporary stabilization of the haem-bound ligand, as is the case in *Vitreoscilla* Hb (Tarricone *et al.*, 1997). Alternatively, other physiological conditions such as the salt concentration may also affect the orientation of the ArgE10 side chain and the presence of the distal water molecules.

3.4. Partial movement of the F-helix C-terminal segment

The structural difference between the Hb structures at neutral pH and other pH conditions is also observed on the proximal side of the haem. Overlapping of these Hb V structures indicated that the C-terminal segment of the F helix shifts toward the FG corner at neutral pH compared with at acidic and alkaline pH (Fig. 3). The displacements of three C-terminal residues of the F helix, GlyF6 to HisF8, are remarkable. The r.m.s.d. of the main-chain atoms of these three residues between the structures at neutral pH and others was approximately 0.81 Å, although the F helix, apart from these three C-terminal residues, overlapped with an r.m.s.d. less than 0.28 Å per pair. The shift of the F helix in Hb V at neutral pH starts at MetF4 and is increased in the flexible region containing GlyF6 and ProF7 (Barlow & Thornton, 1988; Cordes *et al.*, 2002). As a result, although the C-terminus of the F helix displays a 3_{10}-helix or an α-helix at acidic and alkaline pH, the helical conformation is destabilized and stretched at neutral pH.

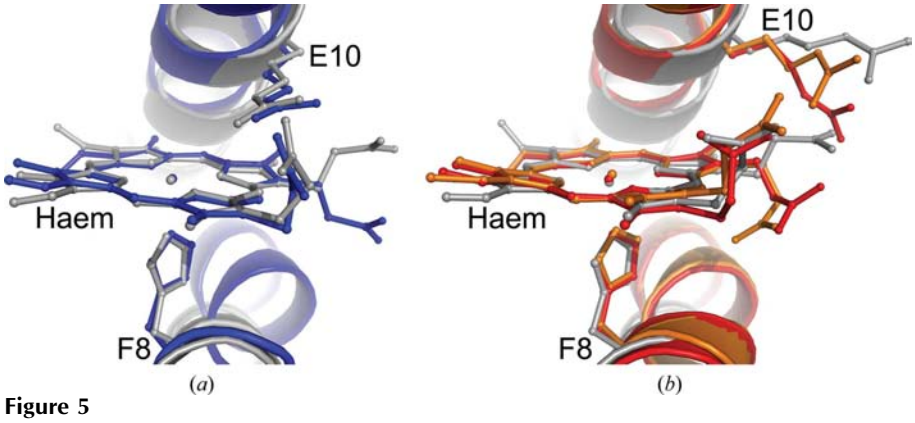

Figure 5
Comparisons of the haem region of *P. akamusi* Hb V and the mollusc *A. limacina* Mb. (*a*) Overlapping of Hb V at pH 7.0 (blue) and the mollusc Mb in the fluoride-bound form (grey). (*b*) Overlapping of Hb V at pH 4.6 (red) and pH 9.0 (orange) and the mollusc Mb in the deoxy form (grey). ArgE10, HisF8 and haem are represented as stick models. Structures were superimposed by overlaying the haem planes.

An overall shift of the F helix associated with the T→R transition has generally been observed in vertebrate Mb and Hb (Baldwin & Chothia, 1979; Perutz, 1979; Paoli *et al.*, 1996; Kachalova *et al.*, 1999). However, the pH-dependent F-helix movement in Hb V is only a partial shift at the C-terminal region and not an overall shift. To date, such a partial shift of the F helix has not been reported in other globin proteins. The pH-dependent conformational change of the F-helix C-terminal segment, which contains HisF8, can lead to haem displacement and can help in determining the haem location and regulation of the functional properties at each pH condition. Structural

comparison of Hb V indicated that the conformational flexibility of the F-helix C-terminal segment is related to the Gly and Pro residues at the F6 and F7 positions, respectively; these residues are known to destabilize helices (Barlow & Thornton, 1988; Cordes *et al.*, 2002). The occurrence of Gly and Pro residues adjacent to HisF8 is extremely rare in the globin proteins, suggesting that these Gly and Pro residues in the F helix were achieved independently in the Hb V lineage. Therefore, partial movement of the F-helix C-terminal segment might be a characteristic mechanism by which the functional properties of *P. akamusi* Hb are maintained.

3.5. Structural changes in the haem region

It is noteworthy how the distal and proximal structural changes affect the location of the haem in Hb V at different pH conditions. In general, the structural changes dependent on haem ligation cause movement of the haem within the globin frame; these changes result in significant changes in the haem geometry in both the pentacoordinate and hexacoordinate globin proteins (Perutz, 1979; Paoli *et al.*, 1996; Kachalova *et al.*, 1999; Riccio *et al.*, 2002; Vallone *et al.*, 2004; de Sanctis *et al.*, 2006). As shown in Table 2, comparison of the geometric parameters indicates that there are no significant differences between all five Hb V structures. However, the overlap model reveals that under acidic and alkaline conditions the haem plane tilts slightly toward the distal side compared with the Hb V structure under neutral conditions, as observed in T-state Hb and Mb (Paoli *et al.*, 1996; Kachalova *et al.*, 1999; Šrajer *et al.*, 2001; Adachi *et al.*, 2003; Bourgeois *et al.*, 2003, 2006; Fig. 3). The movements surrounding the CHA–CHC axis of the haem exhibit 4° and 3° tilts under acidic and alkaline conditions, respectively. Overlapping based on the HisF8 backbone revealed that the haem tilt is associated with the torsion angles of the HisF8 side chain under each pH condition (Fig. 6). This displacement of ligated haem under different pH conditions may contribute to the maintenance of a haem environment that is suitable for ligand affinity under each pH condition. In conclusion, we have described a structural mechanism that leads to haem tilting in Hb V.

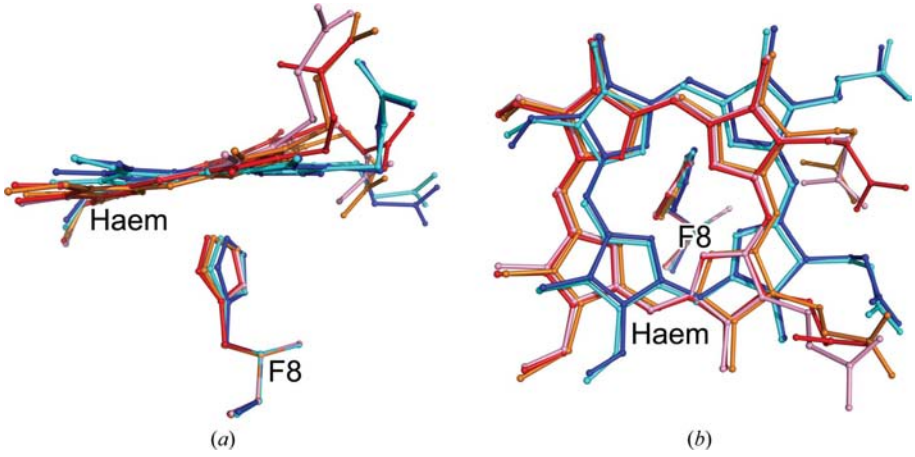

Figure 6
Overlapping of the haem of five Hb V structures based on the HisF8 backbone atoms. (*a*) Side haem view and (*b*) view perpendicular to the haem plane. The coordinates of the Hb V structures at pH 4.6, 5.6, 6.5, 7.0 and 9.0 are presented in red, pink, cyan, blue and orange, respectively. The Fe atom of the haem is deleted from (*b*) for easy viewing.

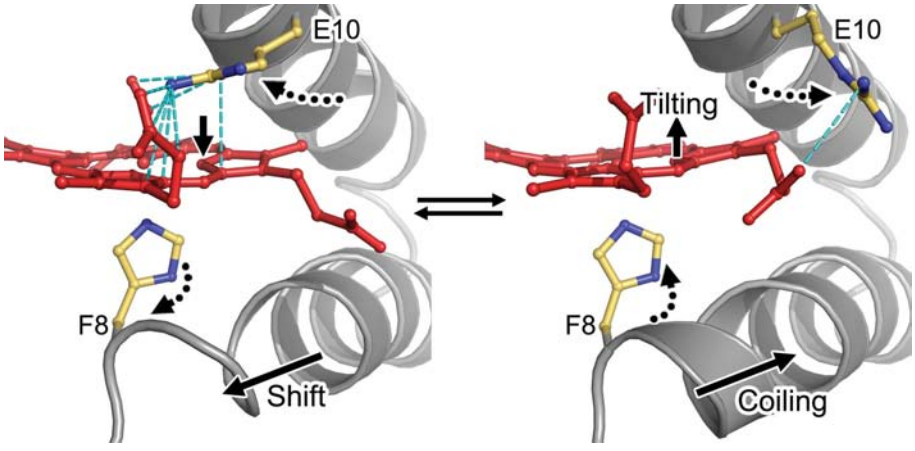

Figure 7
Structural changes in the haem region upon pH change from neutral pH (left) to acidic and alkaline pH (right). Cyan broken lines represent noncovalent bonds, including the hydrogen bonds between the haem and the ArgE10 side chain. Arrows indicated the movements of haem and the F-helix C-terminal segment and dotted arrows imply the movements of the side chain of ArgE10 and HisF8.

Time-resolved structural investigations using photodissociation of CO-bound Hb and Mb have revealed a process of haem tilting (Šrajer *et al.*, 2001; Adachi *et al.*, 2003; Bourgeois *et al.*, 2003, 2006). Bourgeois *et al.* (2006) suggested that the tilting results from variation of strain from the distal Phe residues, which are in close contact with the haem, during CO dissociation-dependent conformational changes. In Hb V, because the movement of the ArgE10 side chain causes a significant change in the noncovalent bonds at the distal side of the haem, the movement probably affects the haem tilting. Interestingly, a survey of PDB entries revealed the occurrence of haem tilting in the mollusc *A. limacina* Mb. In mollusc Mb, the haem in the deoxy and the imidazole-bound forms, in which the ArgE10 side chain swings out from the haem pocket (Conti *et al.*, 1993), tilts approximately 3° toward the distal side compared with that in the fluoride-bound and the cyanide-bound forms, in which the Arg side chain is present on the distal side of the haem (Bolognesi *et al.*, 1990; Mattevi *et al.*, 1991; Conti *et al.*, 1993). These observations suggest that

the movement of ArgE10 is partly responsible for the location of the haem in Hb V.

As illustrated in Fig. 7, we supposed that the pH-dependent haem tilting with the rotation of the HisF8 side chain in Hb Vis induced by the coupled movement of the ArgE10 side chain and the F-helix C-terminal segment. At neutral pH, the Arg side chain can stabilize the haem plane by forming several noncovalent bonds, *i.e.* the side chain exerts a downward force onto the edge of the haem plane. Although the stereochemical clashes between the Arg and the haem may bring about haem displacement with downward rotation of the HisF8 side chain (Fig. 6), the movement of the F-helix C-terminal segment, which is based on GlyF6 and ProF7, appears to cushion these clashes and retain the position of the haem within the frame of the globin fold. Further, the swinging movements of ArgE10 under acidic and alkaline conditions result in a loss of the noncovalent bonds between the haem plane and the Arg, allowing the movement of haem with the upward rotation of the HisF8 side chain. It is considered that under acidic and alkaline conditions noncovalent bonds connecting the haem to the distal side, for example, the hydrogen-bond networks (Figs. 4*a* and 4*c*), pull the haem toward this side. Coupled with the formation of the helical coil in the F-helix C-terminal segment, this increases haem tilting.

It is interesting to observe that the structural changes in the haem region of Hb V are controlled by the movement of ArgE10 and the F helix associated with GlyF6 and ProF7. These amino-acid residues are considered to have been independently acquired by amino-acid substitutions during the evolution of *P. akamusi* Hb V. A large variety of globin proteins with different structures and oxygen-binding properties have been reported. Previous studies have suggested that these structural diversities result from a fine adaptation of the haem environment (Bolognesi *et al.*, 1990, 1997; Mattevi *et al.*, 1991; Conti *et al.*, 1993; Sugimoto *et al.*, 2004). Our observations also indicated that *P. akamusi* Hb V has adapted to the amino-acid substitutions in both the distal and proximal sides of the haem and has achieved a structural mechanism for maintaining its functional properties at each pH condition.

Ligand affinity in globin proteins can be tuned by the haem environment provided in the distal side by gating ligand access to the binding site and by creating or deleting docking sites and cavities within the protein moiety (Vallone *et al.*, 2004). In *P. akamusi* Hb V, ArgE10 might play an essential role in tuning the ligand affinity at various pH conditions because its movement directly affects the distal haem environment. Furthermore, the movement of the F-helix C-terminal segment can help determine the haem location according to the movement of the ArgE10 residue. Functional studies of the Hb components of *P. akamusi* indicated that Hb V exhibits acidic and alkaline Bohr effects (Koshikawa *et al.*, 1998; Kamimura *et al.*, 2003; Yamamoto *et al.*, 2003). The autoxidation reaction of oxy-Hb V in both acidic and alkaline pH was quite different from that of another *P. akamusi* Hb component, Hb VII, and that of mammalian Mb containing the usual HisE7 residue (Kamimura *et al.*, 2003). Our structural analyses revealed that the functional changes of Hb V under both acidic and alkaline conditions are controlled by the same molecular mechanism based on the characteristic movement in the haem region of this Hb component.

This work was supported in part by the 'Academic Frontier' Project for Private Universities matching fund subsidy from MEXT, 2000–2004 and 2005–2007 and in part by Nihon University Multidisciplinary Research Grant (2009). We are grateful to all the staff of LEBRA, Nihon University for their helpful technical advice.

References

Adachi, S., Park, S.-Y., Tame, J. R. H., Shiro, Y. & Shibayama, N. (2003). *Proc. Natl Acad. Sci. USA*, **100**, 7039–7044.
Akiyama, K., Fukuda, M., Kobayashi, N., Matsuoka, A. & Shikama, K. (1994). *Biochim. Biophys. Acta*, **1208**, 306–309.
Baldwin, J. & Chothia, C. (1979). *J. Mol. Biol.* **129**, 175–220.
Barlow, D. J. & Thornton, J. M. (1988). *J. Mol. Biol.* **201**, 601–619.
Bolognesi, M., Bordo, D., Rizzi, M., Tarricone, C. & Ascenzi, P. (1997). *Prog. Biophys. Mol. Biol.* **68**, 29–68.
Bolognesi, M., Coda, A., Frigerio, F., Gatti, G., Ascenzi, P. & Brunori, M. (1990). *J. Mol. Biol.* **213**, 621–625.
Bonamore, A., Ilari, A., Giangiacomo, L., Bellelli, A., Morea, V. & Boffi, A. (2005). *FEBS J.* **272**, 4189–4201.
Bourgeois, D., Vallone, B., Arcovito, A., Sciara, G., Schotte, F., Anfinrud, P. A. & Brunori, M. (2006). *Proc. Natl Acad. Sci. USA*, **103**, 4924–4929.
Bourgeois, D., Vallone, B., Schotte, F., Arcovito, A., Miele, A. E., Sciara, G., Wulff, M., Anfinrud, P. & Brunori, M. (2003). *Proc. Natl Acad. Sci. USA*, **100**, 8704–8709.
Collaborative Computational Project, Number 4 (1994). *Acta Cryst.* D**50**, 760–763.
Conti, E., Moser, C., Rizzi, M., Mattevi, A., Lionetti, C., Coda, A., Ascenzi, P., Brunori, M. & Bolognesi, M. (1993). *J. Mol. Biol.* **233**, 498–508.
Cordes, F. S., Bright, J. N. & Sansom, M. S. P. (2002). *J. Mol. Biol.* **323**, 951–960.
Couture, M., Burmester, T., Hankeln, T. & Rousseau, D. L. (2001). *J. Biol. Chem.* **276**, 36377–36382.
DeLano, W. L. (2002). *The PyMOL Molecular Viewer.* http://www.pymol.org.
Fago, A., Hundahl, C., Dewilde, S., Gilany, K., Moens, L. & Weber, R. E. (2004). *J. Biol. Chem.* **279**, 44417–44426.
Fann, Y.-C., Ong, T.-L., Nocek, J. M. & Hoffman, B. M. (1995). *J. Am. Chem. Soc.* **117**, 6109–6116.
Fukuda, M., Takagi, T. & Shikama, K. (1993). *Biochim. Biophys. Acta*, **1157**, 185–191.
Guex, N. & Peitsch, M. C. (1997). *Electrophoresis*, **18**, 2714–2723.
Ikeda-Saito, M., Brunori, M. & Yonetani, T. (1978). *Biochim. Biophys. Acta*, **533**, 173–180.
Kachalova, G. S., Popov, A. N. & Bartunik, H. D. (1999). *Science*, **284**, 473–476.
Kamimura, S., Matsuoka, A., Imai, K. & Shikama, K. (2003). *Eur. J. Biochem.* **270**, 1424–1433.
Knapp, J. E., Bonham, M. A., Gibson, Q. H., Nichols, J. C. & Royer, W. E. Jr (2005). *Biochemistry*, **44**, 14419–14430.
Koshikawa, K., Yamamoto, Y., Kamimura, S., Matsuoka, A. & Shikama, K. (1998). *Biochim. Biophys. Acta*, **1385**, 89–100.
Krell, T., Coggins, J. R. & Lapthorn, A. J. (1998). *J. Mol. Biol.* **278**, 983–997.
Kuwada, T., Hasegawa, T., Sato, S., Sato, I., Ishikawa, K., Takagi, T. & Shishikura, F. (2007). *Gene*, **398**, 29–34.
Laskowski, R. A., MacArthur, M. W., Moss, D. S. & Thornton, J. M. (1993). *J. Appl. Cryst.* **26**, 283–291.

Mattevi, A., Gatti, G., Coda, A., Rizzi, M., Ascenzi, P., Brunori, M. & Bolognesi, M. (1991). *J. Mol. Recognit.* **4**, 1–6.
Milani, M., Pesce, A., Ouellet, Y., Ascenzi, P., Guertin, M. & Bolognesi, M. (2001). *EMBO J.* **20**, 3902–3909.
Milani, M., Savard, P. Y., Ouellet, H., Ascenzi, P., Guertin, M. & Bolognesi, M. (2003). *Proc. Natl Acad. Sci. USA*, **100**, 5766–5771.
Mito, M., Chong, K. T., Miyazaki, G., Adachi, S., Park, S.-Y., Tame, J. R. H. & Morimoto, H. (2002). *J. Biol. Chem.* **277**, 21898–21905.
Olson, J. S., Mathews, A. J., Rohlfs, R. J., Springer, B. A., Egeberg, K. D., Sligar, S. G., Tame, J., Renaud, J.-P. & Nagai, K. (1988). *Nature (London)*, **336**, 265–266.
Olson, J. S. & Phillips, G. N. Jr (1996). *J. Biol. Chem.* **271**, 17593–17596.
Ouellet, H., Milani, M., LaBarre, M., Bolognesi, M., Couture, M. & Guertin, M. (2007). *Biochemistry*, **46**, 11440–11450.
Ouellet, Y. H., Daigle, R., Lagüe, P., Dantsker, D., Milani, M., Bolognesi, M., Friedman, J. M. & Guertin, M. (2008). *J. Biol. Chem.* **283**, 27270–27278.
Ouellet, Y., Milani, M., Couture, M., Bolognesi, M. & Guertin, M. (2006). *Biochemistry*, **45**, 8770–8781.
Paoli, M., Liddington, R., Tame, J., Wilkinson, A. & Dodson, G. (1996). *J. Mol. Biol.* **256**, 775–792.
Perutz, M. F. (1979). *Ann. Rev. Biochem.* **48**, 327–386.
Phillips, S. E. V. (1980). *J. Mol. Biol.* **142**, 531–554.
Phillips, S. E. V. & Schoenborn, B. P. (1981). *Nature (London)*, **292**, 81–82.
Riccio, A., Vitagliano, L., di Prisco, G., Zagari, A. & Mazzarella, L. (2002). *Proc. Natl Acad. Sci. USA*, **99**, 9801–9806.
Robinson, V. L., Smith, B. B. & Arnone, A. (2003). *Biochemistry*, **42**, 10113–10125.
Rohlfs, R. J., Mathews, A. J., Carver, T. E., Olson, J. S., Springer, B. A., Egeberg, K. D. & Sligar, S. G. (1990). *J. Biol. Chem.* **265**, 3168–3176.
Sanctis, D. de, Ascenzi, P., Bocedi, A., Dewilde, S., Burmester, T., Hankeln, T., Moens, L. & Bolognesi, M. (2006). *Biochemistry*, **45**, 10054–10061.
Shaanan, B. (1983). *J. Mol. Biol.* **171**, 31–59.
Smerdon, S. J., Krzywda, S., Brzozowski, A. M., Davies, G. J., Wilkinson, A. J., Brancaccio, A., Cutruzzolá, F., Allocatelli, C. T., Brunori, M., Li, T., Brantly, R. E. Jr, Carver, T. E., Eich, R. F., Singleton, E. & Olson, J. S. (1995). *Biochemistry*, **34**, 8715–8725.
Springer, B. A., Sligar, S. G., Olson, J. S. & Phillips, G. N. Jr (1994). *Chem. Rev.* **94**, 699–714.
Šrajer, V., Ren, Z., Teng, T.-Y., Schmidt, M., Ursby, T., Bourgeois, D., Pradervand, C., Schildkamp, W., Wulff, M. & Moffat, K. (2001). *Biochemistry*, **40**, 13802–13815.
Sugimoto, H., Makino, M., Sawai, H., Kawada, N., Yoshizato, K. & Shiro, Y. (2004). *J. Mol. Biol.* **339**, 873–885.
Tarricone, C., Galizzi, A., Coda, A., Ascenzi, P. & Bolognesi, M. (1997). *Structure*, **5**, 497–507.
Vallone, B., Nienhaus, K., Matthes, A., Brunori, M. & Nienhaus, G. U. (2004). *Proc. Natl Acad. Sci. USA*, **101**, 17351–17356.
Winn, M. D., Isupov, M. N. & Murshudov, G. N. (2001). *Acta Cryst.* D**57**, 122–133.
Yamamoto, Y., Koshikawa, K., Terui, N., Mita, H., Matsuoka, A. & Shikama, K. (2003). *Biochim. Biophys. Acta*, **1652**, 136–143.
Yang, J., Kloek, A. P., Goldberg, D. E. & Mathews, F. S. (1995). *Proc. Natl Acad. Sci. USA*, **92**, 4224–4228.
Yokoyama, T., Chong, K. T., Miyazaki, G., Morimoto, H., Shih, D. T.-B., Unzai, S., Tame, J. R. H. & Park, S.-Y. (2004). *J. Biol. Chem.* **279**, 28632–28640.